

Identification of Potential Phytochemical/Antimicrobial Agents against *Pseudoperonospora cubensis* Causing Downy Mildew in Cucumber through In-Silico Docking

Dr. Manoj kumar

Associate professor, Deptt. of Botany, College of commerce, Arts & Science, Patna

ABSTRACT

Compatibility interactions between the host and the fungal proteins are necessary to successfully establish a disease in plants by fungi or other diseases. Photochemical and antimicrobial substances are generally known to increase plant resilience, which is essential for eradicating fungus infections. Through homology modeling and in silico docking analysis, we assessed 50 phytochemicals from cucumber (*Cucumis sativus*), 15 antimicrobial compounds from botanical sources, and six compounds from chemical sources against two proteins of *Pseudoperonospora cubensis* linked to cucumber downy mildew. Alpha and beta sheets made up the 3D structures of the two protein models. According to Ramachandran plot analysis, the QNE 4 effector protein model was considered high quality because it had 86.8% of its residues in the preferred region. The results of the molecular docking analysis showed that the QNE4 and cytochrome oxidase subunit 1 proteins of *P. cubensis* showed good binding affinities with glucosyl flavones, terpenoids and flavonoids from phytochemicals, antimicrobial compounds from botanicals (garlic and clove) and chemically synthesized compounds, indicating the potential for antifungal activity.

Keywords: phytochemicals; antimicrobial compounds; homology modeling; molecular docking

Introduction

The cucumber crop is widely grown in temperate and tropical regions of the world. It stands in fourth position after tomato (*Lycopersicon esculentum* Mill.), cabbage (*Brassica oleracea* var. *capitata* L.) and onion (*Allium cepa* L.). Cucumber has been considered an essential food source for over 5000 years and is used in culinary and non-culinary products. Fresh fruits are used in salads, pickles, cakes, and cooking. At the same time, processed cucumbers are used in sandwiches. Based on usage, cucumber fruits are divided into two types. "Pickling cucumbers" are mainly used in processing foods such as pickles. "Slicing cucumbers" are used for fresh consumption. Cucumbers are widely used as edible fruits because fruits are crispy, delicious, low in calories, rich in nutrients, and an excellent source of fiber needed for a healthy digestive system. The fruits of cucumbers possess several medicinal properties, namely, preventing constipation, having a cooling effect, and checking jaundice and indigestion [1–4]. Along with these, the consumption of cucumbers also provides good nutritional benefits to human beings.

Every 100 g of cucumber fruit contributes 5 g of carbohydrates, 0.4 g of protein, 0.1 g of fat, 0.3 g of minerals, 10 mg of calcium, 0.4 g of fiber, and traces of vitamin C and iron. Cucumbers are a boon to the cosmetic industry. Many cosmetic products contain cucumber extracts, such as soaps, lotions, creams, and perfumes. In addition, the seeds of cucumbers are used in Ayurvedic preparations [5].

At the global level, about 397 million tons of cucumber were produced from 2,261,318 hectares of land, with average productivity of approximately 19.58 t/ha [6]. In India, 105 metric tons of cucumber was produced from an area of 1673 hectares [7]. Cucumbers are cultivated in several parts of India (Uttar Pradesh, Punjab, Rajasthan, Karnataka, and Andhra Pradesh). Cucumber is prone to several diseases like downy mildew, powdery mildew, fungal and bacterial wilts, and viral infections (cucumber mosaic virus, watermelon bud necrosis virus). It causes more economic losses with regard to production and export. Among these, downy mildew is a primary foliar disease that causes more damage

and devastating losses to cucumber production [8]. Fungal diseases affect the quality and yield of crops. As one of the agricultural limiting diseases, downy mildew on cucumber caused by *P. cubensis* significantly affects cucumber production. Cucumber downy mildew is reported to be found in more than 70 countries around the world. Cucumber downy mildew reduces cucumber yield by 10–20%, or even as much as 40%, without adequate control [9].

Management of *P. cubensis* is challenging because it can overcome the control measures (resistance and fungicide application) very quickly and has long-distance dispersal capacity. More usage of fungicides creates environmental pollution and health hazards. Usually, plants produce primary (proteins and polysaccharides) and secondary metabolites (alkaloids and flavonoids) that play an essential role in defense mechanisms. Phytochemical and antimicrobial compounds are known to boost resistance in plants [10]. Antimicrobial compounds and phytochemicals boost plant defenses by neutralizing fungal effector proteins [11]. Nowadays, researchers are focusing on finding potential phytochemicals or antimicrobial compounds against many plant diseases. The effector proteins manipulate the structure, signaling, and metabolism of the host plant. Oomycetes produce effector proteins and virulence genes for pathogenesis [9]. Recent studies on the genome sequencing of *P. cubensis* and in silico analysis identified the effector proteins which play a role in the pathogenicity or virulence of *P. cubensis* infection. The genome sequencing of *P. cubensis* revealed the presence of 61 effector proteins with sequence similarity to the RXLR motif. The RXLR motif is an effector identified in the oomycetes of *P. cubensis*, the QXLR motif contains an effector designated as QNE. This effector protein plays a major role in the pathogenicity of *P. cubensis*. Genome sequencing of *Pythium insidiosum* revealed the involvement of four genes in pathogenesis viz., Exo-1, 3-beta glucanase, chitin synthase, and cytochrome oxidase subunit 1 [12]. Botanicals have anti-microbial properties and are used against many pathogens, including plant-pathogenic fungi and bacteria. The active compounds or chemical constituents of the botanicals act against pathogens. The botanicals used in this study, i.e., neem, tulsi, pudina, clove, and garlic

are good sources of anti-microbial compounds and are used against many fungal pathogens, especially the oomycetes of fungi [13–17]. Binding interactions between two proteins of *P. cubensis* and ligands derived from *C. sativus* (L.), *Syzygium aromaticum* (L.) Merr. and L.M. Perry, *Ocimum tenuiflorum* (L.), *Allium cepa* (L.), *Mentha arvensis* (L.), and *Azadirachta indica* Juss, and fungicides viz., azoxystrobin, ridomil, kresoxim methyl, curzate and SAR inducers oxalic acid and salicylic acid were studied. Afterwards, molecular docking was carried out using 71 ligands (50 compounds from phytochemicals, 15 antimicrobial compounds, four fungicides, and two SAR inducers) with proteins as receptor targets.

Material and Methods

The protein sequences of *P. cubensis* were downloaded from NCBI using accession numbers (Table 1). The protein modeling for protein sequences was carried out by using SWISS-MODEL (<https://swissmodel.expasy.org>) [18] and the I-TASSER server. The templates were selected from the template identification wizard of SWISS-MODEL and later models were built. The output file was obtained in a PDB format that was used to visualize the model in PyMOL version 2.3 [19].

The SAVES-Procheck server (<https://servicesn.mbi.ucla.edu/SAVES>) (accessed on 28 March 2021) [20] was used to evaluate model quality with Procheck, errat, and verified by 3D Qmean plot. Then, the Ramachandran plot was obtained by Procheck in order to evaluate the model. ProtParam from the EXPASY server (www.expasy.ch/tools) (accessed on 28 March 2021) was [21] used to obtain the physicochemical properties of proteins like theoretical Isoelectric Point (PI), molecular mass, amino acid composition, atomic composition, extinction coefficient, instability index, estimated half-life and aliphatic index.

Template Selection

For each identified template, the template's quality has been predicted from features of the target-template alignment. The templates with the highest quality have then been selected for model building.

Model Building

Models are built based on the target-template alignment using ProMod3 (Studer et al.). Coordinates

which are conserved between the target and the template are copied from the template to the model. Insertions and deletions are remodelled using a fragment library. Side chains are then rebuilt. Finally, the geometry of the resulting model is regularized by using a force field.

Model Quality Estimation

The global and per-residue model quality has been assessed using the QMEAN scoring function.

Ligand Modelling

Ligands present in the template structure are transferred by homology to the model when the following criteria are met: (a) The ligands are annotated as biologically relevant in the template library, (b) the ligand is in contact with the model, (c) the ligand is not clashing with the protein, (d) the residues in contact with the ligand are conserved between the target and the template. If any of these four criteria is not satisfied, a certain ligand will not be included in the model. The model summary includes information on why and which ligand has not been included.

Oligomeric State Conservation

The quaternary structure annotation of the template is used to model the target sequence in its oligomeric form. The method is based on a supervised machine learning algorithm, Support Vector Machines, which combines interface conservation, structural clustering, and other template features to provide a quaternary structure quality estimate. The QSQE score is a number between 0 and 1, reflecting the expected accuracy of the interchain contacts for a model built based a given alignment and template. Higher numbers indicate higher reliability. This complements the GMQE score which estimates the accuracy of the tertiary structure of the resulting mode.

Ligands' Source and Fungal Receptor Proteins

The phytochemicals present in *C. sativus*, antimicrobial compounds from botanicals viz., *Ocimum tenuiflorum*, *Allium cepa*, *Syzygium aromaticum*, *Azadirachta indica*, and *Mentha arvensis*, and fungicides were obtained from the published literature [22–28]. A total of 71 compounds were selected for molecular docking, details of these compounds are given in Table 2. The three-dimensional (3D) structures of proteins were obtained from the protein data bank (www.rcsb.org) Similarly, 3D confirmers of the selected ligands were retrieved from the

PubChem(<https://pubchem.ncbi.nlm.nih.gov>) (accessed on 25 March 2021 database in PDB and SDF formats, respectively).

Preparation of Ligands and Target Proteins

Using Avogadro version 1.2.0 [29] with force field type MMFF94, the ligands' 3D structures were optimized and then translated to PDB format using Open Babel version 3.1.1. Further simplification was attained by running the optimized ligands with the lowest energy through the AutoDock-MGL tools [30], adding the Gasteiger charges, and obtaining the PDBQT files via standard processes. A PyMOL check of the downloaded 3D structures was made to check for side-chain anomalies, improper bonds, and missing hydrogens [19]. Using Biovia Discovery Studio 2020, all water molecules, ions, complex molecules of ligands, and proteins were removed [31]. APDB structure was optimized with Auto Dock-MGL by adding the polar hydrogens to obtain the PDBQT files.

Active Site Prediction and Molecular Docking

Using Biovia Discovery Studio 2020, the active sites of fungal proteins were determined. Molecular docking of optimized ligands and proteins in PDBQT format was performed using Auto Dock Vina software [30]. Auto Dock Vina software uses its scoring function (binding affinity) to predict the interaction between ligand and protein. A grid box of $60 \text{ \AA} \times 60 \text{ \AA} \times 60 \text{ \AA}$ was used for proteins with different XYZ coordinates based on predicted active sites for molecular docking. After docking analysis, the output file consists of the top nine binding poses, with their respective binding affinity in kcal/mol. The ligand binding poses with the highest binding affinity and the lowest root mean square deviation (RMSD) were chosen. The protein-ligand interaction in 3D structure was visualized in Py-MOL. The two-dimensional (2D) structure was also visualized in Biovia Discovery Studio 2020. The 3D visualization indicates the target protein's binding pocket or precise location. On the other hand, the 2D structure visualization shows the different bonds formed between the amino acid residues of the fungal target protein and ligand. The workflow of molecular docking of compounds with proteins of *P. cubensis* associated with cucumber is depicted in Figure 1. The botanicals studied in molecular docking were further evaluated under in vitro conditions.

Result

Table 1.

Table 1. Protein sequences retrieved from National Centre for Biotechnology Information (NCBI)

Sequence Description	Length of Proteins	Sequence of Amino Acids
Cytochrome oxidase subunit 1 of <i>P. cubensis</i> (Accession No. AEA38564.1)	412	MNFQNIKNWSTRWLFSTNHHKDIGTXYLIFSAFAGIVG TTLSILIRIELAQPGNQIFMGNHQLYNVVVTAHAFVMV FFLVMPALIGGFGNWFVPLMIGAPDMAFPRMNNISFW LLPPALLLLISSAIVESGAGTGWAVYPPSSVQAHSGPS VDLAIFSLHLTGISLLGAINFISTIYNMRAPGLSFHRLPL FVWSILITAFLLLLTLPVLAGAITMLLTDRNLNTSFYDPS GGGDPVLYQHLFWFFGHPEVYVYLILPAFGIISQVSAYFA KKNVFGYLGVMYAMLSIGLLGSIVWAHHMFTVGLDVD TRAYFSAATMIIAVPTGIKIFSWLATLWGGSLKFETPLLF TLGFILLFVMGGVTGVVMSNSGLDIALHDYYIVGHFH YVLSMGAIFGIFTGFYFWIGKISGRR
QNE 4 effector protein <i>P. cubensis</i> (Accession No. ADW27474.1)	517	MMPPAKLVAYIAVASSIVLARYEASTDITSTSDANKLSIS APSDPVQHDTKQLLRTSDTAVTKDNEERMFNAAGLKR ASTMSHFADVHGLPHEPLAPHLHDTYDPAGASHPPVLP YTGEAKAHEDLQHAASTSNPLKKISPADTQLTEGENNE AEILKRIMTLMQPVAPRALKRKRKLPDGTETQLQWNE SDILDYKHKDKFLNIMNEWLNLGPGQAFERMILEN QLPTSIYEDYVMFHAAKDEEMYEHFQKQNEGILPKEI EEKINAVLPKARKAPLVVRLNKYEVFYKQPFAYR TKLLDEDEPEEAERLKSCKWDRLRVVLKVRSSQRKTK FTLQWFRKHPNEFLLKSIQEGTPPEDIRSVLGLARLEGL KLFKHPNYEYLLKYLKLFQTHSTEHWQERVPKGMPP EDVRFILGLGQLKGSEFSQHPNFPEYIKFFELWHEAYTRK KMKEWMQLNTPLEAFKLAIRDHNDVEFIVDKSDLY MKQYENEWKKKHPTLRTPAVST

Cytochrome c oxidase subunit 1

The document lists the results for the homology modelling project “subunit 1” submitted to **SWISS-MODEL** workspace on April 4, 2024, 6:50 A.M. The submitted primary amino acid sequence is given in Table T1. The SWISS-MODEL template library (SMTL version 2024-03-27, PDB release 2024-03-22) was searched with for evolutionary related structures matching the target sequence in Table T1. For details on the template search, see Materials and Methods. Overall 550 templates were found (Table T2).

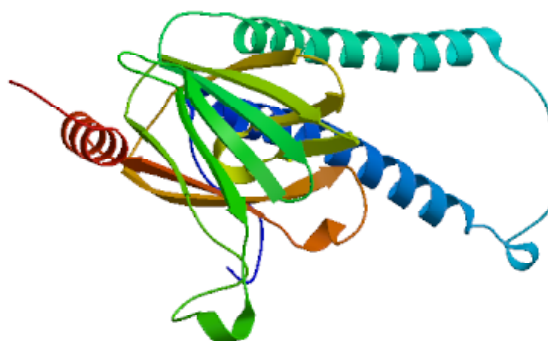
Models

Fig: model was built

Built with	Oligo-State	Ligands	GM QE	Template	Seq Identity	Found by	Method	Seq Similarity	Range	Coverage	Description
ProMod3 3.4.0	monomer	None	0.94	AF-F2YQF3-F1-model-v4	99.17	AFDB search	AlphaFold v2	0.61	1-241	1.00	Cytochrome c oxidase subunit 1

The template contained no ligands.

Target

Epwqlgfdpatpvmegiinfhhdliiflvvtvfvewmlrvitlfdkknkipatvvhgatieiwtspalilliva

F2yqf3.1. Aepwqlgfdpatpvmegiinfhhdliiflvvtvfvewmlrvitlfdkknkipatvvhgatieiwtspalilliva

Target Ipsfallysmdevidpiitlkvigsqwywsyeydsnlfsdeplvfdsymvqeddlaigqfrilevdrvvvptnshirv

f2yqf3.1. aipsfallysmdevidpiitlkvigsqwywsyeydsnlfsdeplvfdsymvqeddlaigqfrilevdrvvvptnshirv

Target litasdvhlswaipslgikldacpgrlnqtsmfikregvfygqseicgvnhgmpivveavsledyliwlknkinfdfn

F2yqf3.1. alitasdvhlswaipslgikldacpgrlnqtsmfikregvfygqseicgvnhgmpivveavsledyliwlknkinfdfn

Target i

F2yqf3.1.ai

Table t1:

Primary amino acid sequence for which templates were searched and models were built.

Epwqlgfdpatpvmegiinfhhdliiflvvtvfvewmlrvitlfdkknkipatvvhgatieiwtspalillivaipsfall

Ysmdevidpiitlkvigsqwywsyeydsnlfsdeplvfdsymvqeddlaigqfrilevdrvvvptnshirv litasdvhlswaipslgikld

Cpgrlnqtsmfikregvfygqseicgvnhgmpivveavsledyliwlknkinfdfn

Table T2:

Template	Seq Identity	Oligostate	Found by	Method	Resolution	Seq Similarity	Coverage	Description
F2YQF3.1.A	99.17	Monomer	AFDB search	AlphaFold v2	NA	0.61	1.00	Cytochrome c oxidase subunit 1
7jro.1.B	65.68	Monomer	BLAST	EM	NA	0.51	0.98	Cytochrome c oxidase subunit 1
7jro.1.B	65.53	Monomer	HHblits	EM	NA	0.51	0.98	Cytochrome c oxidase subunit 1
8c8q.1.B	50.85	Monomer	HHblits	EM	NA	0.45	0.97	Cytochrome c oxidase subunit 1

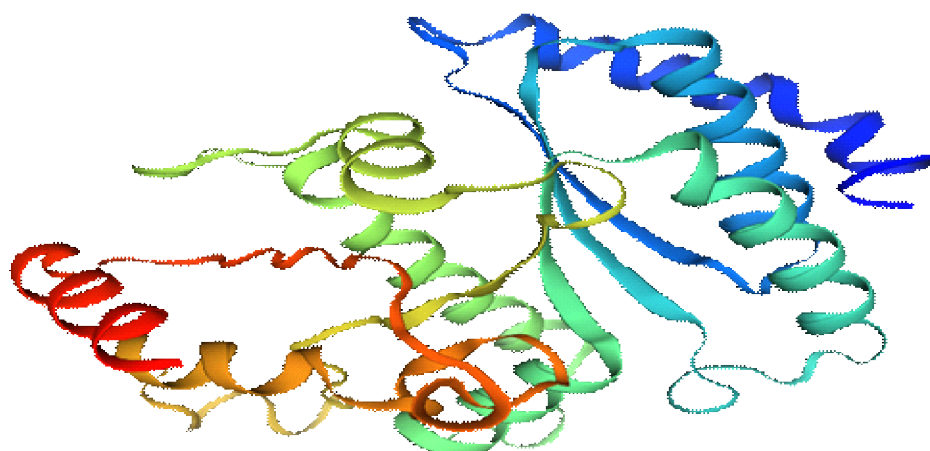
8c8q.1.B	51.72	Monomer	BLAST	EM	NA	0.46	0.96	Cytochrome c oxidase subunit 1
6t0b.1.V	53.68	Monomer	BLAST	EM	NA	0.46	0.96	Cytochrome c oxidase subunit 1
6hu9.1.V	53.68	Monomer	BLAST	EM	NA	0.46	0.96	Cytochrome c oxidase subunit 1
6t15.1.V	53.68	Monomer	BLAST	EM	NA	0.46	0.96	CYTOCHROME C OXIDASE SUBUNIT 1 SYNONYM: CYTOCHROME C OXIDASE POLYPEPTIDE II, COX2
7z10.1.B	53.68	Monomer	BLAST	EM	NA	0.46	0.96	Cytochrome c oxidase subunit 1
6ymy.1.B	53.68	Monomer	BLAST	EM	NA	0.46	0.96	Cytochrome c oxidase subunit 1

2. QNE 4 effector protein

This document lists the results for the homology modelling project “QNE 4 effector protein” submitted to SWISS-MODEL workspace on April 4, 2024, 7:07 a.m. The submitted primary amino acid sequence is given in Table T1. The SWISS-MODEL template library (SMTL version 2024-03-27, PDB release 2024-03-22) was searched with for evolutionary related structures matching the target sequence in Table T1. For details on the template search, see Materials and Methods. Overall 6970 templates were found (Table T2).

Models

Fig: model was built



The following model was built (see Materials and Methods “Model Building”):

Built with	Oligo-State	Ligands	GM QE	Template	Seq Identity	Found by	Method	Seq Similarity	Rang e	Coverage	Description
ProMold3 3.4.0	monomer	None	0.94	AF-11TGK8-F1-model-v4	100.00	AFDB search	AlphaFold v2	0.62	1-231	1.00	QNE 4 effector protein chain

The template contained no ligands

Target kglytegaelidsvldvrkeaesdclqgfqithslgggtgsgmgtlliskireypdrimctysvcpspkvsdtvvep
 i1tgk8.1.akglytegaelidsvldvrkeaesdclqgfqithslgggtgsgmgtlliskireypdrimctysvcpspkvsdtvvep
 Target ynatlsvhqlvenadevmcldealydicfrtklttptygdlnhlvcaamsgittclrfpgqlnsdlrklavnlpfpr
 i1tgk8.1.aynatlsvhqlvenadevmcldealydicfrtklttptygdlnhlvcaamsgittclrfpgqlnsdlrklavnlpfpr
 Target lhffmigfapltsgsqyraltpeltqqqfdaknmcaadprhgryltaacmfrgrmstkevdeqmlnl
 i1tgk8.1.alhffmigfapltsgsqyraltpeltqqqfdaknmcaadprhgryltaacmfrgrmstkevdeqmlnl

Table t-1:

Primary amino acid sequence for which templates were searched and models were built
 Kglytegaelidsvldvrkeaesdclqgfqithslgggtgsgmgtlliskireypdrimctysvcpspkvsdtvvepynatlsvhqlvenadevmcldealydicfrtklttptygdlnhlvcaamsgittclrfpgqlnsdlrklavnlpfprlhffmigfapltsgsqyraltpeltqqqfdaknmcaadprhgryltaacmfrgrmstkevdeqmlnl

Table-2

	Seq Identity	Oligostate	Found by	Method	Resolution	Seq Similarity	Coverage	Description
I1TGK8.1.A	100.00	Monomer	AFDB search	AlphaFold v2	NA	0.62	1.00	QNE 4 effector protein chain
8g3d.121.A	93.51	Monomer	BLAST	EM	NA	0.59	1.00	QNE 4 effector protein chain
8g2z.243.A	93.51	Monomer	BLAST	EM	NA	0.59	1.00	QNE 4 effector protein chain
8g3d.247.A	93.51	Monomer	BLAST	EM	NA	0.59	1.00	QNE 4 effector protein chain
7mwg.1.B	93.51	Monomer	BLAST	EM	NA	0.59	1.00	QNE 4 effector protein chain
6u42.5.A	90.91	Monomer	BLAST	EM	NA	0.59	1.00	QNE 4 effector protein
6u42.39.A	90.91	Monomer	BLAST	EM	NA	0.59	1.00	QNE 4 effector protein
6u42.15.A	90.91	Monomer	BLAST	EM	NA	0.59	1.00	QNE 4 effector protein
7n61.133.A	90.91	Monomer	BLAST	EM	NA	0.59	1.00	QNE 4 effector protein
6u42.24.A	90.91	Monomer	BLAST	EM	NA	0.59	1.00	QNE 4 effector protein

Table 2.

List of ligands such as terpenoids, glucosyl flavones, flavonoids, megastigmane derivatives, indolic secondary metabolites, flavone glucosides, polyphenols, antimicrobial compounds, and chemically synthesized compounds used for molecular docking analysis.

Group	Sl. No.	Compounds	tbChem/Drug Bank ID	Source
Terpenoids	1	Cucurbitacin-A	5281315	<i>Cucumis sativus</i> L.
	2	Cucurbitacin-B	5281316	<i>Cucumis sativus</i> L.
	3	Cucurbitacin-C	5281317	<i>Cucumis sativus</i> L.
	4	Cucurbitacin-D	5281318	<i>Cucumis sativus</i> L.
	5	Cucurbitacin-E	5281319	<i>Cucumis sativus</i> L.
	6	Cucurbitacin-I	5281321	<i>Cucumis sativus</i> L.
Glucosyl flavones	7	Cucumerin-A	44257649	<i>Cucumis sativus</i> L.
	8	Cucumerin-B	44257648	<i>Cucumis sativus</i> L.
Flavonoids	9	Vitexin	5280441	<i>Cucumis sativus</i> L.
	10	Isovitexin	162350	<i>Cucumis sativus</i> L.
	11	Orientin	5281675	<i>Cucumis sativus</i> L.
	12	Isoorientin	114776	<i>Cucumis sativus</i> L.
Megastigmane derivatives	13	Cucumegastigmane-I	16105430	<i>Cucumis sativus</i> L.
	14	Cucumegastigmane-II	16105434	<i>Cucumis sativus</i> L.
	15	(+)-Dehydrovomifoliol	688492	<i>Cucumis sativus</i> L.
Indolic secondary metabolites	16	Indole-3-aldehyde	10256	<i>Cucumis sativus</i> L.
	17	Indole-3-carboxylic acid	69867	<i>Cucumis sativus</i> L.
Flavone glucosides	18	Isoscoparin	442611	<i>Cucumis sativus</i> L.
	19	Saponarin	441381	<i>Cucumis sativus</i> L.
	20	Vicenin-2	442664	<i>Cucumis sativus</i> L.
	21	Apigenin-7- <i>O</i> -glucoside	5280746	<i>Cucumis sativus</i> L.
	22	Quercetin-3- <i>O</i> -glucoside	5280804	<i>Cucumis sativus</i> L.
	23	Isorhamnetin-3- <i>O</i> -glucoside	5318645	<i>Cucumis sativus</i> L.
	24	Kaemferol-3- <i>O</i> -rhamnoside	5316673	<i>Cucumis sativus</i> L.
Polyphenol	25	4-hydroxycinnamic acid	637542	<i>Cucumis sativus</i> L.
Antimicrobial compounds	26	Carrageenan	71597331	<i>Acanthophora specifira</i> V.
	27	Acyclovir	135398513	Chemically synthesized
	28	5-Azacytidine	9444	Chemically synthesized
	29	Cytarabine	6253	Chemically synthesized
	30	Ribavirin	37542	Chemically synthesized
	31	Ridovudine	35370	Chemically synthesized
	32	Ningnanmycin	44588235	<i>Streptomyces noursei</i> var. <i>xichangensis</i>
	33	Vidarabine	21704	Chemically synthesized
	34	Acycloguanosine	135398513	Chemically synthesized
	35	2-Thiouracil	1269845	Chemically synthesized
	36	Moroxydine hydrochloride	76621	Chemically synthesized
	37	Luotonin A	10334120	<i>Peganum nigella</i> strum B.
	38	Tylophorinine	264751	<i>Cynanchum</i> , <i>Pergularia</i> and

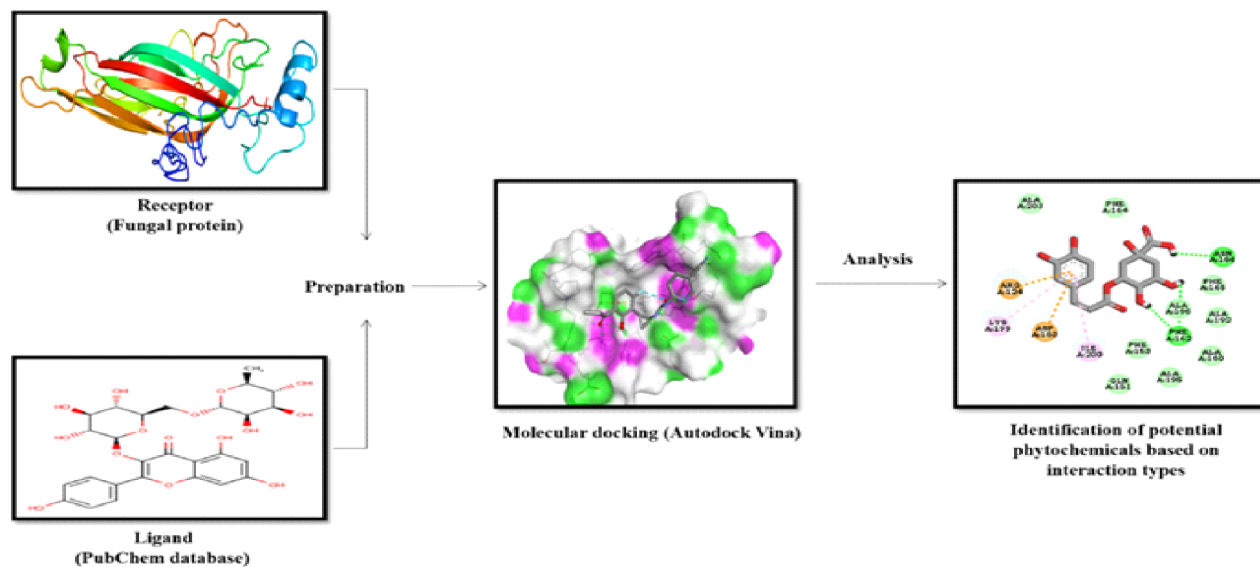


Figure 1. The workflow of molecular docking analysis of phytochemicals, antimicrobial compounds, and chemically synthesized compound agents with proteins of *P. cubensis*.

Table 3. Linear combination of two structural descriptors for model quality assessment.

Sl. No.	Protein	Template	Query Coverage (%)	Per Cent Similarities (%)	GMQE	QMEAN
1	Cytochrome oxidase subunit 1	7 jro 1. B	99	99.0	0.77	0.67
2	QNE 4	5 gnc 1. A	100	93.94	0.16	0.43 +/- 0.05

Table 4. Calculated secondary structures (in percentage) by SOPMA.

Secondary Structures	QNE4	Cytochrome Oxidase Subunit 1
Alpha helix %	42.36	44.77
Extended strand %	12.38	21.17
Beta turn %	8.70	8.27
Random coil %	36.56	25.79

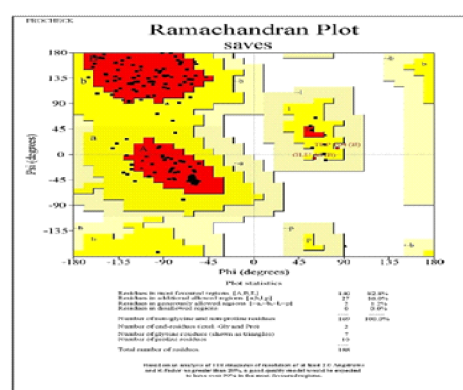
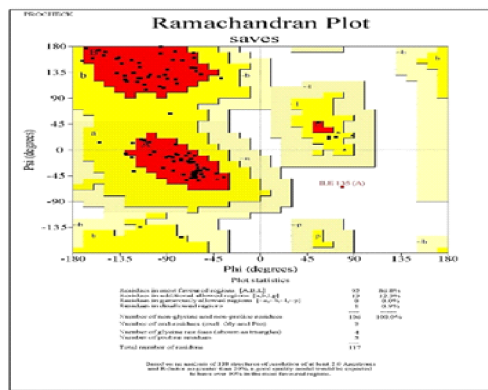
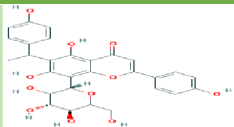
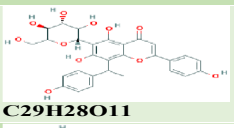
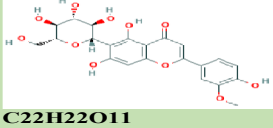
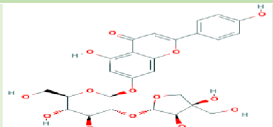
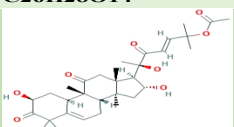
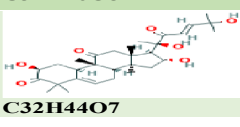


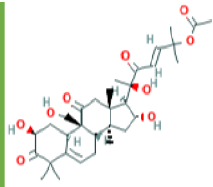
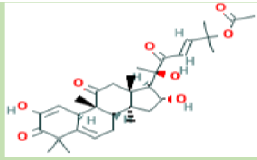
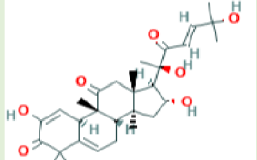
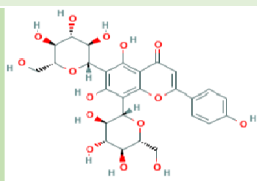
Figure 2. Comparative protein model quality assessment by using a Ramachandran plot for (a) QNE4 and (b) cytochrome oxidase subunit 1 proteins.

Table 5. Ramachandran plot statistics for QNE4 and cytochrome oxidase subunit 1 proteins.

Ramachandran Plot Statistics	QNE4 Residues	QNE4 Percentage	Cytochrome Oxidase Subunit 1 Residues	Cytochrome Oxidase Subunit 1 Percentage
Residues in most favored regions [A, B, L]	92	86.8	140	82.8
Residues in additional allowed regions [a, b, l, p]	13	12.3	27	16.0
Residues in generously allowed regions [~a, ~b, ~l, ~p]	0	0.0	2	1.2
Residues in disallowed regions	1	0.9	0	0.0
Number of non-glycine and non-proline residues	106	100.0	169	100.0
Number of end-residues (except Gly and Pro)	2		2	
Number of glycine residues (shown in triangles)	4		7	
Number of proline residues	5		10	
Total number of residues	117		188	

Table 6. Number of hydrogen bonds formed during the interaction between top phytochemicals/antimicrobial compound structures with the QNE 4 effector protein of *P. cubensis* associated with cucumber.

Sl. No.	Compound with PubChem ID	Structural Formula	No. of H Bonds	Amino Acid Residue of QNE 4 Effector Protein Involved in Hydrogen Bonding with Ligand
1	Cucumerin-A 44257649	 C29H28O11	4	ARG339, TVR290, LEU 126, ASN134
2.	Cucumerin-B 44257648	 C29H28O11	1	HIS110
3	Isoscoparin 442611	 C22H22O11	3	SER109, HS110, GLY217
4	Apigenin-7-Oglucoside 5280746	 C26H28O14	4	ASN214, SER109, MET224, GLY107
5	Cucurbitacin-B 5281316	 C32H46O8	1	HIS110
6	Cucurbitacin-D 5281318	 C32H44O7	3	SER 125, TYR108, ARG146

7	icurbitacin-A 5281315		2	SER140, SER82
		C32H46O9		
8	icurbitacin-E 5281319		2	SER 82, SER 109
		C32H44O8		
9	ucurbitacin-I 5281321		3	LYS121, GLS127, ARG339
		C30H42O7		
10	Vicenin-2 442664		4	SER109, HIS83, GLY107, SER82
		C27H30O15		

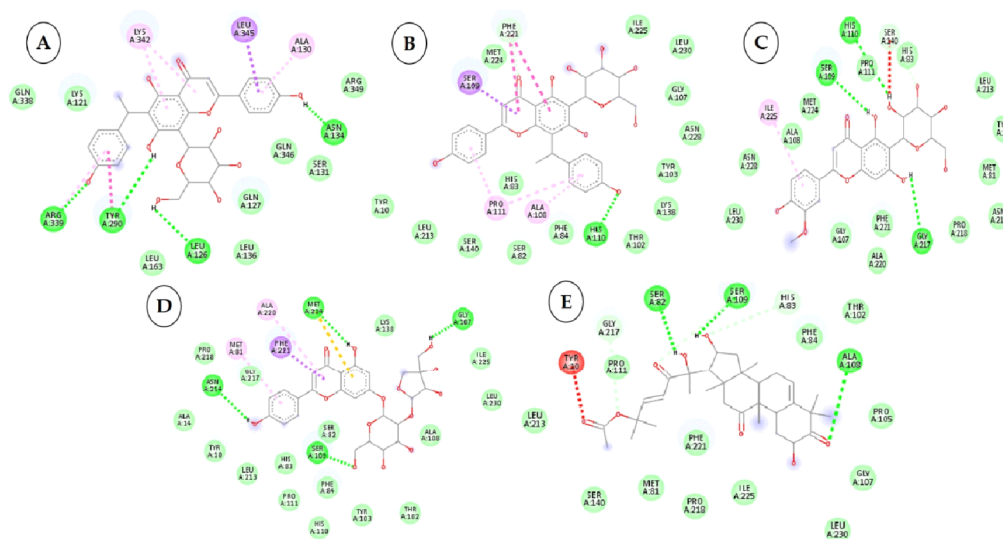


Figure 3. Two-dimensional visualization of the interaction between the QNE 4 effector protein and the top five phytochemicals (A) Cucumerin A (B) Cucumerin B (C) Isocarpin (D) Apigenin-7-Oglucoside (E) Cucurbitacin-B.

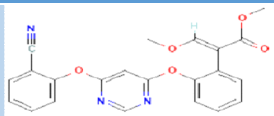
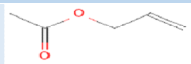
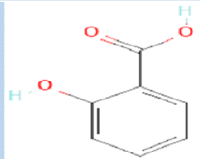
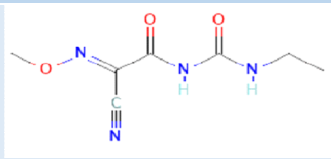
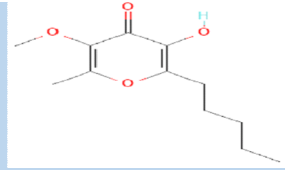
Sl. No.	Compound with PubChem ID	Structural Formula and Chemical Formula	No. of H Bonds	Amino Acid Residue of QNE4 Effector Protein Involved in Hydrogen Bonding with Ligand
1	Zoxystrobin 3034285	 C ₂₂ H ₁₇ N ₃ O ₅	1	SER109
2	Allyl acetate 11584	 C ₅ H ₈ O ₂	2	ASP86, HIS83
3	Salicylic acid 338	 C ₇ H ₆ O ₃	3	ALA376, ARG377, LEU381
4	Curzate 5364079	 C ₇ H ₁₀ N ₄ O ₃	4	THR456, ALA376
5	Allixin 86374	 C ₁₂ H ₁₈ O ₄	2	ARG285, GLN165

Table 7. The number of hydrogen bonds formed during the interaction between top antimicrobial compounds from botanicals and chemically synthesized compound structures with the QNE4 effector protein of *P. cubensis* associated with cucumber

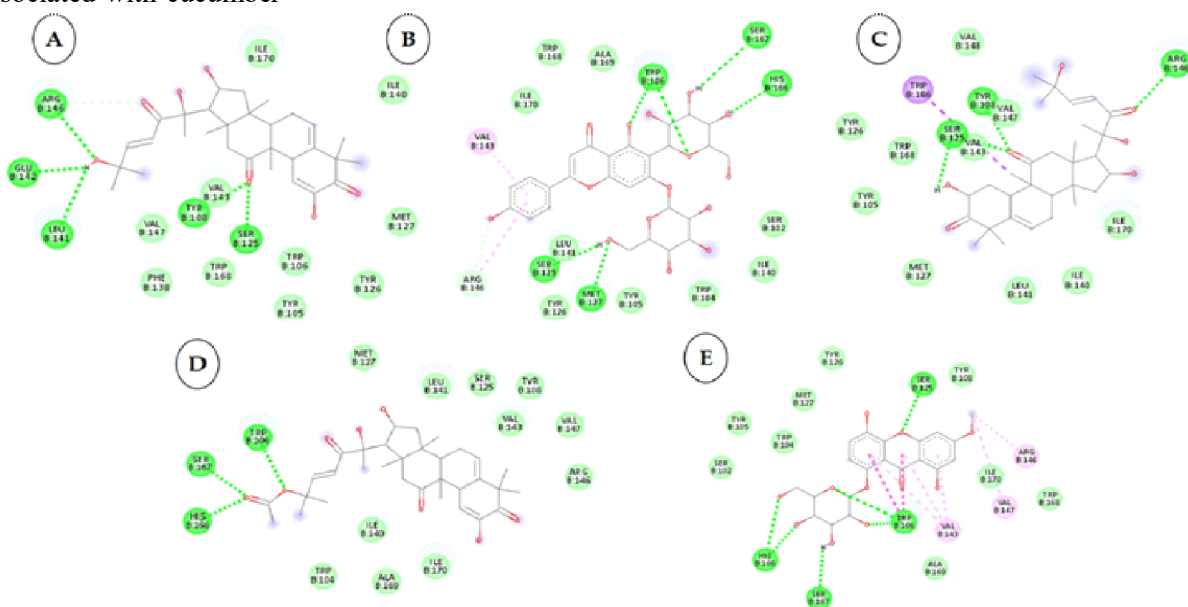


Figure 4. Two-dimensional visualization of the interaction between the cytochrome oxidase subunit1 protein and the top five phytochemicals (A) Cucurbitacin-I (B) Saponarin (C) Cucurbitacin-D (D) Cucurbitacin-E (E) Swertianolin S.

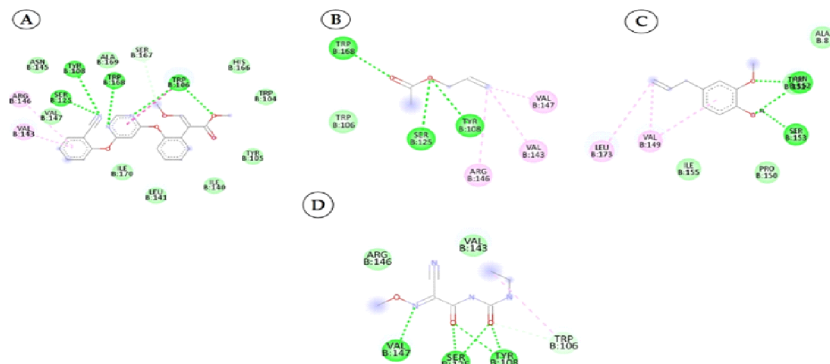


Figure 5. Two-dimensional visualization of the interaction between the cytochrome oxidase subunit 1 protein and top compounds from botanicals and chemical sources (A) Azoxystrobin (B) Allyl acetate (C) Kresoxim methyl (D) Curzate.

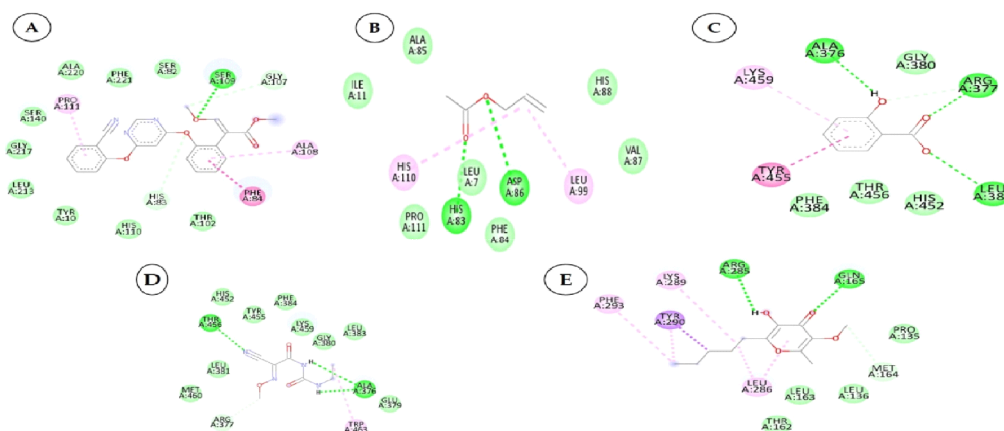


Figure 6. Two-dimensional visualization of the interaction between the QNE 4 effector protein and top compounds from botanicals and chemical sources (A) Azoxystrobin (B) Allyl acetate (C) Salicylic acid (D) Curzate (E) Allixin.

Table 8. Number of hydrogen bonds formed during the interactions between top phytochemicals/antimicrobial compound structures and the cytochrome oxidase subunit 1 protein of *P. cubensis* associated with cucumber.

Sl. No.	Compound with PubChem ID	Structural Chemical Formula	No. of H Bonds	Amino Acid Residue of Cytochrome Oxidase Subunit 1 Protein Involved in Hydrogen Bonding with Ligand
1	ucurbitacin-I 5281321	 C30H42O7	5	ARG461, GLU142, LEU141, TYR108, SER125
2	Saponarin 441381	 C22H30O15	5	TRP106, SER167, HIS166, SER125, MET127
3	ucurbitacin-D 5281318	 C32H44O7	3	ARG146, TYR108, SER125

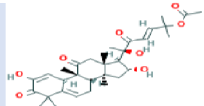
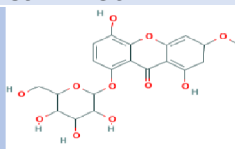
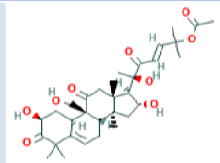
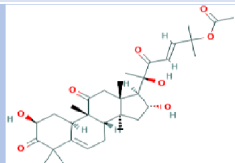
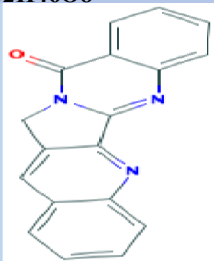
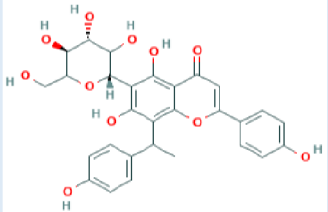
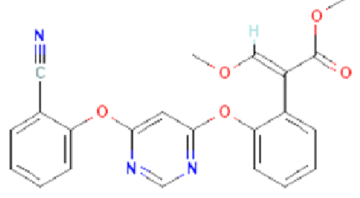
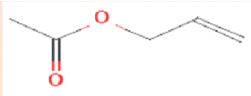
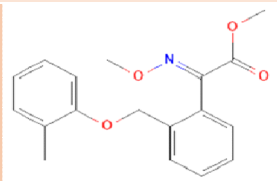
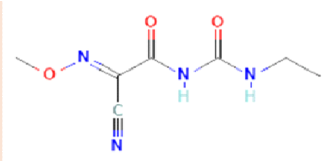
4	ucurbitacin-E 5281319	 C32H44O8	3	TRP106, SER167, HIS166
5	Swertianolin 5858086	 C20H20O11	4	SER125, HIS166, SER167, TRP106
6	ucurbitacin-A 5281315	 C32H46O9	5	TRP168, SER125, SER167, HIS166, TRP104
7	ucurbitacin-B 5281316	 C32H46O8	5	ASN152, ARG146, LEU141, VAL145, VAL147
9	Luotonin 10334120	A  C18H11N3O	2	TYR108, SER125
10	Cucumerin-B 44257648	 C29H28O11	5	LEU141, MET127, SER125, TYR108, SER167

Table 9. Number of hydrogen bonds formed during the interaction between top antimicrobial compounds from botanicals and chemically synthesized compound structures and the cytochrome oxidase sub-unit 1 protein of *P. cubensis* associated with cucumber

Sl. No.	Compound with PubChem ID	Structural and Chemical Formula	No. of H Bonds	Amino Acid Residue of Cytochrome Oxidase Subunit 1 Protein Involved in Hydrogen Bonding with Ligand
1	zoxytrobin 3034285	 C22H17N3O5	4	SER125, TYR108, TRP168, TRP106

2	llyl acetate 11584	 C5H8O2	3	SER125, TYR108 and TRP168
3	esoxim methyl 6112114	 C18H19NO4	2	TAM 552, SER153
4	Curzate 5364079	 C7H10N4O3	3	VAL147, SER125, TYR108

Discussion:

Modeling and Physicochemical Properties of Proteins

Prediction of the 3D Structure of Proteins of *P. cubensis*

The two protein sequences of *P. cubensis* were obtained and annotated (Table 1). The BLASTn results showed high query coverage (>99%) and percent identity (>99.47%) in both the proteins of *P. cubensis*. Later, these sequences were selected for protein modeling using SWISS-MODEL.

Template Selection

The selection of templates for building homology models was performed using the wizard of SWISS-MODEL with the following criteria: the template should show high coverage, i.e., >65 percent of the target aligned to the template and sequence identity should be more than 30 percent. Then, we used the GMQE and QMEAN scoring functions as initial criteria to discriminate good models from bad. Higher GMQE and QMEAN scores and acceptable alignment values were obtained during modeling, suggesting that statistically acceptable homology models were generated [37]. The output file was obtained in a PDB format that was used to visualize the model in PyMOL version 2.3. [19]. Global model quality estimation (GMQE) is the quality estimation that combines properties from the target-template alignment. The quality estimate ranges between 0 and 1 with higher values for better models. Qualitative model energy analysis (QMEAN) is a composite scoring function describing the major geometrical aspects of protein structures (Table 3).

Ramachandran Plot Analysis

The Ramachandran plot indicated the phi-psi torsion angle for all residues in the structure (except those at the chain termination). The darkest areas correspond to the 'core' region representing the most favorable combinations of phi-psi values. Ideally, one would hope to have over 90 percent of the residues in these 'core' regions. The percentage of residues in the 'core' region is one of the best guides to stereo-chemical quality. A good quality Ramachandran plot has over 90 percent in the most favored region [38].

Ramachandran plot analysis was carried out for two proteins (cytochrome oxidase subunit 1 and QNE4) of *P. cubensis*. The QNE4 effector protein was shown to have 86.8 percent of residues in the favored region (red color), 12.3 percent in the additionally allowed area (yellow color), 0 percent of residues in the generously allowed region (beige color), and 0.9 percent of residues in the disallowed region (white color) (Figure 2a). Similarly, the cytochrome oxidase subunit 1 protein had 82.8 percent of residues in the favored region (red color), 16.0 percent in the additionally allowed region (yellow color), 1.2 percent of residues in the generously allowed region (beige color), and 0 percent of residues in the disallowed region (white color) (Table 5) (Figure 2b). Homology modeling plays a vital role in structural proteomics and developing or designing potential compounds using an in silico approach.

Physico-Chemical Properties of Two Proteins of *P. cubensis*

The physico-chemical properties of proteins of *P. cubensis* were determined by ProtParam from the

EXPASY server (www.expasy.ch/tools) (accessed on 28 March 2021) [21] and furnished in Table 6. The extinction coefficient indicates how much light a protein absorbs at a particular wavelength. The instability index estimates the protein's stability in a test tube. If it is greater than 40, it is not stable; hence the effector QNE4 protein was stable in nature and another protein, cytochrome oxidase subunit 1, was unstable in nature. The grand average of hydropathic (GRAVY) value, which is calculated as the sum of the hydropathic values of all the amino acids divided by the number of residues in the sequence. A negative GRAVY value indicates that the protein is non-polar and a positive value indicates that the protein is polar. Hence, our results revealed that both proteins are non-polar in nature (Table 6). The overall stereochemical properties of the generated models were highly reliable and valuable in understanding the protein function.

Molecular Docking Studies

To develop effective phytochemicals/antimicrobial compounds from botanicals against *P. cubensis* associated with cucumber, approximately 71 compounds from plant and chemical sources were used for molecular docking with proteins as a potential target. Before the docking analysis, the ligands were optimized by minimizing the energy with force field type MMFF94, and this helps in removing clashes among atoms and developing a stable starting pose of the ligands for binding interaction [39].

The docking, coupled with a scoring function, can be utilized to screen a large number of potential phytochemicals in silico. Generally, in molecular docking, a binding affinity lower than the upper threshold (≤ 6 kcal/mol) is considered the cut-off value for concluding good binding affinity between protein and ligand [39]. The 3D and 2D visualization of phytochemicals, antimicrobial compounds, and chemically synthesized compounds based on binding affinity with respective fungal receptor proteins has been represented (Supplementary Figures S1–S6), (Figures 3–6). Hydrogen bond energy majorly contributed to the score [40] of selected compounds used in the current molecular docking studies against two proteins of *P. cubensis*, which displayed very good dock scores above the threshold cut-off of ≤ 6 kcal/mol (Table 7). The ligand structures and necessary hydrogen bond formation between the top phytochemicals, antimicrobial compounds, and fungicides with their respective fungal protein receptors have been illustrated in Tables 8–11.

Interactions between the QNE4 Effector Protein and Phytochemicals, Antimicrobial Compounds, and Chemically Synthesized Compounds

Molecular docking analysis of QNE 4 with 50 phytochemicals showed that the majority of the compounds bind to the effector protein of *P. cubensis* with favorable binding energies ranging from ≤ 4.4 kcal/mol (for Indole-3-aldehyde) to ≤ 9.1 kcal/mol (cucumerinA), whereas antimicrobial compounds from different botanical sources and fungicides showed binding energies in the range of ≤ 3.4 to ≤ 12.1 (Table 7). Among the 50 phytochemicals, cucumerin-A (≤ 9.1 kcal/mol), Isocarpin (≤ 8.5 kcal/mol), apigenin-7-O-glucoside (≤ 8.5 kcal/mol), cucumerin-B (≤ 8.5 kcal/mol), cucurbitacin-B (≤ 8.3 kcal/mol), cucurbitacin-D (≤ 8.2 kcal/mol), cucurbitacin-A and cucurbitacin-E (≤ 8.1 kcal/mol), cucurbitacin-I (≤ 8.0 kcal/mol), vincein (≤ 8.0 kcal/mol), and caragenin (≤ 8.0 kcal/mol) were the top 10 compounds with the highest binding affinities.

The phytochemical compounds belonging to glucosyl flavones, terpenoids, and flavonoids have shown an excellent inhibitory action on the QNE4 effector protein of *P. cubensis*. Among the 15 antimicrobial compounds from botanicals tested, azoxystrobin (≤ 8.1 kcal/mol), allyl acetate (≤ 7.2 kcal/mol), (E)- β -caryophyllene (≤ 6.8 kcal/mol), salicylic acid (≤ 6.5 kcal/mol), curzate (≤ 6.0 kcal/mol), and allixin (≤ 5.8 kcal/mol) showed highest binding affinities (Table 7). The antimicrobial compounds obtained from botanicals namely, garlic and clove have shown a good inhibitory action on QNE4 effector protein of *P. cubensis*. At the same time, azoxystrobin (≤ 8.1 kcal/mol), salicylic acid (≤ 6.5 kcal/mol) and curzate (≤ 6.0 kcal/mol) are the chemical compounds which exhibited the highest binding affinities. Overall, cucumerin-A (≤ 9.1 kcal/mol) showed good inhibitory action on the QNE4 effector protein of *P. cubensis* out of 71 compounds tested.

Among the phytochemical compounds, cucumerin-A (≤ 9.1 kcal/mol) exhibited the highest docking score with the QNE 4 effector protein. The ARG339, TVR290, LEU126, ASN134 amino acid residue is involved in forming four hydrogen bonds in the binding pocket of the QNE 4 effector protein.

cucurbitacin-A interacted with two hydrogen bonds, the LYS121, GLN127, and ARG339 amino acids of cucurbitacin-I contributed three hydrogen bonds, vicenin-2 created an interaction with the SER109, HIS83, GLY107, and SER82 amino acids and generated

four hydrogen bonds, and carrageenan interacted with the SER109, PHE84, HIS83, and HIS110 amino acids by forming four hydrogen bonds with the binding of the QNE4 effector protein of *P. cubensis* (Table 8).

In binding interactions between 15 antimicrobial compounds from different botanicals and six compounds from chemical sources and QNE 4, the docking score ranged from “3.4 to “8.1. Out of 21 compounds, the azoxystrobin (“8.1 kcal/mol) chemical compound showed the top docking score with the QNE 4 effector protein and interacted with SER109 amino acid residues to form one hydrogen bond in the binding pocket of the QNE 4 effector protein. Likely, allyl acetate created an interaction with the ASP86 and HIS83 amino acids and produced two hydrogen bonds; three hydrogen bonds of the ALA376, ARG377, and LEU381 amino acids were generated upon interaction with salicylic acid, the THR456 and ALA376 amino acids of curzate were involved in forming two hydrogen bonds, and the ARG285 and GLN165 amino acids shared two hydrogen bonds with allixin with the QNE4 effector protein of *P. cubensis* (Table 9).

Interactions between the Cytochrome Oxidase Subunit 1 Protein and Phytochemicals

Antimicrobial Compounds, and Fungicides

Among the 50 phytochemicals used for screening against the cytochrome oxidase subunit 1 protein, Indole-3-aldehyde has shown the lowest dock score of 4.4 kcal/mol and cucurbitacin-I have shown the highest dock score of 8.3 kcal/mol (Table 7). Ten compounds; cucurbitacin-I (“8.3 kcal/mol), saponarin (8.1 kcal/mol), cucurbitacin-D (8.0 kcal/mol), swertianolin (8.0 kcal/mol), cucurbitacin-E (8.0 kcal/mol), cucurbitacinA (7.9 kcal/mol), cucurbitacin-B (7.8 kcal/mol), cucumerin-A (7.8 kcal/mol), luotonin.A (7.8kcal/mol), and cucumerin-B (7.7 kcal/mol) exhibited better dock scores. The phytochemicals from terpenoids, glucosyl flavones, and the flavone glucosides group have shown good affinities with the target cytochrome oxidase subunit 1 protein of *P. cubensis*.

Cucurbitacin-I interacted with the ARG461, GLU142, LEU141, TYR108, and SER125 amino acid residues through forming five hydrogen bonds with the cytochrome oxidase subunit 1 protein of *P. cubensis*. Likewise, the TRP106, SER167, HIS166, SER125, and MET127 amino acids of catechin shared five hydrogen bonds, cucurbitacin-D displayed an interaction with the ARG146, TYR108, and SER125 amino acids and produced three hydrogen bonds, three hydrogen bonds of the TRP106, SER167, and HIS166 amino acids were generated upon interactions with

cucurbitacin-E, swertianolin created an interaction with the SER125, HIS166, SER167, and TRP106 amino acids and developed four hydrogen bonds, the TRP168, SER125, SER167, HIS166, and TRP104 amino acids of cucurbitacin-A were involved in forming five hydrogen bonds, cucurbitacin-B interacted with the ASN152, ARG146, LEU141, VAL145, and VAL147 amino acids by forming five hydrogen bonds, the LEU141, SER125, TRP106, and SER167 amino acids of cucumerin- A contributed four hydrogen bonds, Luotonin A interacted with the TYR108 and SER125 amino acids by forming two hydrogen bonds, and cucumerin-B interacted with the LEU141, MET127, SER125, TYR108, and SER167 amino acids by forming five hydrogen bonds with the active site of the cytochrome oxidase subunit 1 protein.

The docking score for the 21 antimicrobial compounds and fungicides ranged from “3.2 kcal/mol (for azadiractin b) to 7.2 kcal/mol (for azoxystrobin). Four compounds; azoxystrobin (7.2 kcal/mol), allyl acetate (6.6 kcal/mol), kresoxim methyl (6.3 kcal/mol), and curzate (5.3 kcal/mol) exhibited uppermost binding affinities (Table 7). The compounds from chemical sources and antimicrobial compounds from garlic showed superior affinities with the target cytochrome oxidase subunit 1 protein of *P. cubensis*. Azoxystrobin interacted with the SER125, TYR108, TRP168, and TRP106 amino acid residues in forming four hydrogen bonds with the cytochrome oxidase subunit 1 protein of *P. cubensis*. Similarly, the SER125, TYR108, and TRP168 amino acids shared three hydrogen bonds with allyl acetate, and two hydrogen bonds of the TAM 552 and SER153 amino acids were interfaced with kresoxim methyl. The VAL147, SER125, and TYR108 amino acids of curzate contributed three hydrogen bonds with the active sites of the cytochrome oxidase subunit 1 protein of *P. cubensis*.

Conclusion:

In the present investigation, glucosyl flavones (cucumerin A, cucumerin B), terpenoids (cucurbitacin-A, cucurbitacin-B, cucurbitacin-C, cucurbitacin-D, cucurbitacin-E, and cucurbitacin-I), flavanone glucosides (isocarpin, apigenin-7-O-glucoside, vicenin-2, and saponarin), and antimicrobial compounds (luotionin) have shown good binding interactions on the ONE4 and cytochrome c oxidase subunit 1 proteins of *P. cubensis*. Similarly, luotonin-A has shown broad-spectrum fungicidal activities against 14 different phytopathogenic fungi.

Among the botanicals tested, antimicrobial compounds from garlic (allyl acetate, allicin, and alliin) and clove (eugenol acetate and (E)- α -caryophyllene) showed an excellent binding affinity with the ONE4 and cytochrome c oxidase subunit 1 proteins of *P. cubensis*. It was reported that the alliin from garlic showed significant binding interactions with the target-Avr3a11 effector protein of *Phytophthora capsici* compared to the commonly used fungicides, indicating that alliin can act as a potential inhibitor of Avr3a11. It was revealed that chemical compounds from garlic have antioxidant properties by conducting molecular docking analysis of the chemical compounds of garlic against NADPH oxidase.

The best docking score obtained on NADPH oxidase corresponds to α bisabolol ($G = 10.62$ kcal/mol), followed by 5-methyl-1, 2, 3, 4-tetrathiane ($G = 9.33$ kcal/mol). In silico analysis of eugenol against the α -glucosidase effector protein of *Fusarium solani* f. sp. *piperis* revealed that eugenol showed promising fungicidal activity and cytotoxic activity similar to that of tebuconazole fungicide. α -glucosidase showed good binding interaction with eugenol by forming amino acid residues with Arg177 followed by a hydrogen bond with Glu596, indicating an essential role in the interactions and justifying the antifungal action of this compound.

Out of the six chemically synthesized compounds evaluated, oxalic acid, salicylic acid, azoxystrobin, and curzate showed good binding interactions with the effector proteins of *P. cubensis*. Likewise, the results were studied earlier through molecular docking studies of the cytochrome b gene of *Peronospora litchi*, the causal agent of litchi downy mildew. The results showed that salicylic acid has more binding affinity and interaction with the PR1 protein. Among the five botanicals tested, garlic bulb extract showed maximum inhibition (71.42%) followed by clove oil (64.51%). Garlic bulb extract at a 15 percent concentration showed maximum inhibition of sporangial germination (71.42%), followed by clove oil at a 5 percent concentration (71.76%). Results from earlier reports found that the concentrations of 50–1000 $\mu\text{g/ml}$ allicin in garlic juice reduced the severity of cucumber downy mildew caused by *P. cubensis* by approximately 50–100 per cent under controlled conditions. The volatile antimicrobial substance allicin from garlic (*Allium sativum*) at concentrations 50–100 $\mu\text{g/mL}$ reduced the severity of *P. cubensis* on cucumber by approximately 50–100%. In addition, clove oil at 4 percent effectively reduced the downy mildew incidence in cucumber.

The phytochemical compounds belonging to glucosyl flavones, terpenoids and flavonoids have shown good binding interactions on the ONE4 effector protein of *P. cubensis*. Among the five botanicals tested, garlic bulb extract showed maximum inhibition (71.42%), followed by clove oil (64.51%). However, it is important to evaluate the phytochemicals and chemically synthesized compounds under in vitro and in vivo conditions and botanicals under in vivo conditions to validate the prediction studies as many phytochemicals and chemically synthesized compounds have a potential role in the inhibition of *P. cubensis* in cucumber

References:

1. Agrios GN. Plant pathology. 5th ed. London: Elsevier 2005, 427-33.
2. Akem C, Jovicich E. Integrated management of foliar diseases in vegetable crops. Project Number: VG07127. Horticulture Australia Ltd, Brisbane, Queensland 2013.
3. Babadoost M, Richard AW, John BM. Identifying and managing cucurbit pests: Diseases, insects, and weeds. University of Illinois Extension, 2004, 48.
4. Berkeley MS, Curtis A. *Peronospora cubensis*. Botanical Journal of the Linnean Society. 1868;10:363.
5. Bernhardt E. Cucurbit diseases: A Practical guide for seedsmen, growers & agricultural advisors. Petoseed Co., Saticoy, CA, 1988, 48.
6. Boregowda N, Puttaswamy H, Harischandra SP, Nagaraja G. Trichoderma oligosaccharides priming mediates, resistance responses in pearl millet against downy mildew pathogen. Journal of Applied Biology and Biotechnology. 2017;5(2):97-103.
7. Brzozowski L, Holdsworth WL, Mazourek M. 'DMRNY401': A new downy mildew-resistant slicing cucumber. Hort Science. 2016;51:1294-1296.
8. Choi YJ, Hong SB, Shin HD. A re-consideration of *Pseudoperonospora cubensis* and *P. humuli* based on molecular and morphological data. Mycological Research. 2005;109:841-848.
9. Cohen Y. The combined effects of temperature, leaf wetness, and inoculum concentration on infection of cucumbers with *Pseudoperonospora cubensis*. Canadian Journal of Botany. 1977; 55:1478-1487.

10. Dong JL, Jae-Sung L, Young-Joon C. Co-Occurrence of two phylogenetic clades of *Pseudoperonospora cubensis*, the causal agent of downy mildew disease, on oriental pickling melon. *Mycobiology*. 2021;49(2):188-195.
11. Gent DH, Mitchell MN, Holmes GJ. Genetic and pathogenic relatedness of *Pseudoperonospora cubensis* and *P. humuli*: Implications for detection and management. *Phytopathology*.
12. Göker M, Voglmayr H, Riethmüller A, Oberwinkler F. How do obligate parasites evolve? A multi-gene phylogenetic analysis of downy mildews. *Fungal Genetics and Biology*. 2007;44:105-122.
13. Goldenhar KE, Hausbeck MK. Fungicides for control of downy mildew on pickling cucumber in Michigan. *Plant Health Progress*. 2019;20:165-169.
14. Holmes G, Ojiambo P, Hausbeck M, Quesada-Ocampo L, Keinath A. Resurgence of cucurbit downy mildew in the United States: A watershed event for research and extension. *Plant Disease*. 2015;99:428-441.
15. Iwata Y. Specialization in *Pseudoperonospora cubensis* (Berk. et Curt.) Rostov. II. Comparative studies of the morphologies of the fungi from *Cucumis sativus* L. and *Cucurbita moschata* Duchesne. *Annals of the Phytopathological Society of Japan*. 1942;11:172-185.
16. Keinath AP. Utility of a cucumber plant bioassay to assess fungicide efficacy against *Pseudoperonospora cubensis*. *Plant Disease*. 2016;100:490-499.
17. Keinath AP, Wintermantel WM, Zitter TA. *Compendium of cucurbit diseases and pests*. Second Edition. USA: American Phytopathological Society publication, 2017, 222
18. Lebeda A, Cohen Y. Cucurbit downy mildew biology, ecology, epidemiology, host-pathogen interaction and control. *European Journal of Plant Pathology*.
19. Lebeda A, Widrechner MP. A set of Cucurbitaceae taxa for differentiation of *Pseudoperonospora cubensis* pathotypes. *Journal of Plant Diseases and Protection*. 2003;110:337-349.
20. Mitchell MN, Ocam C, Gent D. Addressing the relationship between *Pseudoperonospora cubensis* and *Pseudoperonospora humuli* by multigenic characterization and host specificity. *Phytopathology*. 2009;99:S87.
21. Mohamed A, Hamza A, Derbalah A. Recent approaches for controlling downy mildew of cucumber under greenhouse conditions. *Plant Protection Sciences*. 2016;52(1):1-9.
22. Palti J, Cohen Y. Downy mildew of cucurbits (*Pseudoperonospora cubensis*): The fungus and its hosts, distribution, epidemiology, and control. *Phytoparasitica*. 1980;8:109-147.
23. Patel JS, Wyenandt CA, McGrath MT. Effective downy mildew management in basil using resistant varieties, environment modifications, and fungicides. *Plant Health Progress*. 2021;22:226-234.
24. Porchas M, Matheron ME. Comparison of fungicides for management of downy and powdery mildew on lettuce. *Plant Disease Management Reports*. 2010;5:V129.
25. Rahman A, Miles T, Martin F, Quesada-Ocampo L. Molecular approaches for biosurveillance of the cucurbit downy mildew pathogen, *Pseudoperonospora cubensis*. *Canadian Journal of Plant Pathology*. 2017;39(3):282-296.
26. Rajni SS, Pandya RK, Pramod KF. Management of pearl millet downy mildew by the application of bioagents, chemicals and botanical. *International Journal of Chemical Studies*. 2018;6(1): 606-608.
27. Runge F, Thines M. A potential perennial host for *Pseudoperonospora cubensis* in temperate regions. *European journal of plant pathology*. 2009;123(4), 483-486.
28. Runge F, Thines M. Reevaluation of host specificity of the closely related species *Pseudoperonospora humuli* and *P. cubensis*. *Plant Disease*. 2012;96:55-61.
29. Runge F, Ndambi B, Thines M. Which morphological characteristics are most influenced by the host matrix in downy mildews? A case study in *Pseudoperonospora cubensis*. *Plos One*. 2012;7(11)
30. Salcedo A, Purayannur S, Standish JR, Miles T, Thiessen L, Quesada-Ocampo LM. Fantastic downy mildew pathogens and how to find them: Advances in detection and diagnostics. *Plants*. 2021;10:435.
31. Savory EA, Granke LL, Quesada Ocampo LM, Varbanova M, Hausbeck MK, Day B. The cucurbit downy mildew pathogen *Pseudoperonospora cubensis*. *Molecular Plant Pathology*. 2011;12(3):217-226.

